Regular Article

ANALYTICAL AND BIOANALYTICAL CHEMISTRY RESEARCH

Published by the Iranian Chemical Society

Anal. Bioanal. Chem. Res., Vol. 5, No. 1, 95-114, June 2018.

Removal of Brilliant Green and Crystal violet from Mono- and Bi-component Aqueous Solutions Using NaOH-modified Walnut Shell

Motahare Ashrafi, Ghadamali Bagherian*, Mansour Arab Chamjangali and Nasser Goudarzi

Faculty of Chemistry, Shahrood University of Technology, Shahrood, P. O. Box: 36155-316, Iran

(Received 18 November 2017, Accepted 16 January 2018)

In the present work, the simultaneous determination of Brilliant green (BG) and Crystal violet (CV) dyes with overlapped absorption spectra in binary mixture solution was carreid out using the partial least squares (PLS) and direct ortogonal signal correction-partial least squares (DOSC-PLS) methods. The results obtained indicate that applying DOSC on the calibration and prediction data for each dye leads to the significantly minimized error prediction. Walnut shell, as an abundant lignocellulosic agricultural waste, was modified using NaOH, and subsequently characterized by the Fourier transform-infrared (FT-IR) spectroscopy, scanning electron microscopy (SEM) and BET techniques. The potential application of the prepared adsorbent for the removal of the cited dyes was investigated. The effects of the experimental parameters such as the initial pH, adsorbent dosage, initial dye concentration, and contact time on the adsorption efficiency in the single solutions and their binary mixture were also studied. The optimum experimental conditions were found to be 0.8 g l^{-1} of the adsorbent at room temperature, pH 7.0, and a contact time of 13 min. These advantages fascilitate the dye removal. The analysis data shows that the Langmuire isotherm can satisfactorily explain the equilibrium data. The maximum adsorption capacity (q_m) for BG and CV in their single solutions was found to be 146.40 and 123.2 mg g^{-1}, respectively, whereas these values for their binary mixture were 79.07 and 96.01 mg g^{-1}, respectively. The exhausted NMWNS was regenerated using a dish-washing liquid and reused for removal of the cited dye species from aqueous solutions.

Keywords: Removal, Partial least squares regression, Signal correction, Cationic dyes

INTRODUCTION

Nowadays more than one hundred thousand kinds of commercial dyes are utilized with an annual production of over nine million tones [1]. A large amount of these dyes are lost during manufacturing and dying procedures, which produce a large amount of dye-containing wastewaters [2]. Brilliant green (BG) and Crystal violet (CV) are two kinds of cationic dyes that are extensively used in the printing ink, paper, plastic, leather, textile, silk, and wool industries. Also they are employed as biological stains and dermatological agents in medicine [3]. In spite of the commercial importance of BG and CV, the major problems associated with these colored effluents are their toxic, carcinogenic, and mutagenic effects and skin sensitivity and eye diseases [3-5]. In addition, they affect the photosynthesis process in aquatic environments by decreasing the sunlight penetration and dissolved oxygen [6]. Consequently, it is essential to decolorize the effluents containing these compounds prior to their mixing-up with natural water. To date, different techniques have been proposed by different researchers for the treatment of wastewaters polluted with colored effluents [6,7]. Due to the simplicity of design, insensitivity of toxic substances, and availability and ability to treat dyes, the adsorption of pollutants using eco-friendly materials is a

*Corresponding author. E-mail: Gh_Bagherian@shahroodut.ac.ir

powerful and convenient technology with respect to the other techniques [5,7,8]. Activated carbon is the most widely used adsorbent for this purpose [7,9]. It is capable of adsorbing many dyes with a high adsorption capacity [5]. However, activated carbon is often produced from expensive and valuable materials like wood or coal, whose regeneration is costly [2,7,9,10]. This problem has caused the application of low-cost resources such as natural materials and waste materials from industry and agriculture for the removal of dyes [7]. Due to their abundant, low cost, and appropriate adsorption capacity, agricultural waste has been appearing in the adsorption processes [10]. Walnut shell (WNS), an abundant agricultural residue (with a production rate of 290,000 tons per year in Iran) [11] with a large specific surface area and good chemical stability [12], has been successfully used for the removal of single-component aqueous solutions such as malachite green and Lanaset Red [12,13]. However, in the application of adsorption for purification of the industrial effluents, the solution often includes more than one dye. The interaction between these compounds may mutually enhance or reduce the adsorption capacity [2]. Therefore, it is important to study the simultaneous removal of dyes. To the best of our knowledge, there is no report in the literature on the adsorption capacity of NaOH-modified walnut shell (NMWNS) in mixture systems. Therefore, the aim of this work was to investigate the performance of the prepared adsorbent for the removal of BG and CV from single and binary solutions. In order to investigate the adsorption behavior of a dye mixture, it is necessary to determine the concentrations of the dyes in a dye mixture simultaneously [2]. Among the most widely used analytical methods, the spectrophotometric techniques are cheaper and simpler. However, overlapping absorption peaks limit the use of the traditional spectrophotometric techniques [2]. Fortunately, the multivariate calibration methods such as partial least squares (PLS) method expand the applicability of spectrophotometric methods for multi-component analysis [14]. The advantage of a multi-component analysis using multivariate calibration is its speed in the determination of the components present in a mixture, avoiding the preliminary separation step [15]. Partial least squares regression (PLSR) is of particular interest because, unlike multiple linear regression (MLR), it can be used to analyze the data with strongly collinear (correlated), noisy, and numerous X-variables [16]. Another advantage of PLS is that this method can be performed by ignoring the concentration of all the other components except for the analyte of interest [17]. This method requires a calibration set, where the relationship between the spectra (X) and the component concentration (Y) is realized from a set of reference samples, followed by a prediction step in which the results obtained from the calibration are used to determine the component concentrations using the sample UV-Vis spectrum [14,18].

Pre-processing data before calibration often improves the calibration model by filtering the strongly structured (*i.e.* systematic) variation in X that is not correlated to Y [18]. Differentiation and signal correction are two types of pre-processing techniques commonly reported in the literature [19]. Since all of these methods have some problems [20,2], Westerhuis *et al.* [22] have introduced direct orthogonal signal correction (DOSC) as a signal correction technique to remove the variation that is unrelated (*i.e.* orthogonal) to Y (the vector that has to be modeled (*e.g.* concentration)) from the spectra as much as possible [23]. DOSC is a suitable pre-processing method for PLS calibration of mixtures without loss of prediction capacity [17,18]. After the DOSC correction, a new PLS model can be built that is less complex than the model built with the original, uncorrected data [23].

To the best of our knowledge, the application of this pre-processing technique has not yet been reported in the literature for the simultaneous analysis of dye mixtures with the overlapped peaks. Therefore, for the first time, the PLS algorithm was used for the resolution of binary mixtures of the cited dyes. The results obtained with and without using the DOSC algorithm (as a pre-processing technique of the original data) were compared. Then, adsorption of the cited dyes onto NMWNS was investigated. The influence of the experimental factors such as the solution pH, adsorbent dosage, initial dye concentration, and contact time on the adsorption capacity was studied in a batch mode, and various isotherms were evaluated to model the equilibrium data. Finally, the mechanism of the adsorption process and the reusability of the adsorbent were investigated.

EXPERIMENTAL

Materials, Instruments and Software

WNS was removed manually from walnut fruit supplied from a supermarket, Shahrood, Iran. CV (molecular formula = $C_{25}H_{30}N_3Cl$, molecular weight = 407.89, maximum wavelength = 590 nm) and BG (molecular formula = $C_{27}H_{33}N_2HO_4S$, molecular weight = 482.64, maximum wavelength = 624 nm) were supplied from Merck and used without further purification. 0.200 g l^{-1} of the stock solution of each dye (CV and BG) was prepared, and the required diluted solutions were prepared daily by diluting the appropriate volumes of their stock solutions with doubly distilled water. The pH measurements were made using a Metrohm 744 pH-meter equipped with a combined glass electrode. In order to record the UV-Vis spectra (in a wide range of wavelengths from 200 to 800 nm), a double-beam UV-Vis spectrophotometer (Rayleigh UV-2601) was used. The surface features and functional groups of NMWNS were investigated using a scanning electron microscope (SEM) (KYKY-EM3200), a Field Emission scanning electron microscope (FESEM) (MIRAW TESCAN), and a Fourier transform infrared (FT-IR) spectrophotometer (WQF-520), respectively. A BET surface analyzer (Belsorp-Max, BEL, Japan Inc.)) was used for examining the N_2 adsorption-desorption isotherms at 77 K. The PLS and DOSC programs were written in the MATLAB (Mathworks Inc) software and run on a personal computer.

Batch Dye Adsorption Studies

Dye adsorption studies were performed by mixing a known amount of the adsorbent with 50 ml of the dye solutions of definite concentrations in a series of 100-ml beakers in single and binary systems. The pH values for these solutions were adjusted by addition of either HCl (0.1 M) or NaOH (0.1 M). The beakers were agitated using a magnetic stirrer at 200 rpm at 25 ± 2 °C to investigate the effects of pH, adsorbent dosage, and initial dye concentration on the percentage dye removal. Then, at a pre-selected time interval, a certain amount of the sample (2 ml) was centrifuged at 3500 rpm for 1 min. The dye concentration in the supernatant solution was analyzed spectrophotometrically. The BG and CV concentrations in the binary solution were determined using the PLS method.

The individual percentage removal (R, %) and the adsorbed amount of each dye per weight of the adsorbent at equilibrium ($q_{e,i}$) can be calculated using Eqs. (1) and (2), respectively:

$$R = \frac{(C_{0,i} - C_{e,i})}{C_{0,i}} \times 100 \quad (1)$$

$$q_{e,i} = \frac{(C_{0,i} - C_{e,i})V}{W} \quad (2)$$

where $C_{0,i}$ is the initial dye concentration (mg l^{-1}), $C_{e,i}$ is the residual dye concentration at equilibrium (mg l^{-1}), V is the volume of the solution (l), and W is the mass of the dry adsorbent used (g).

Preparation of Adsorbent

WNS was ground in a domestic grinder and washed for several times with distilled water until the supernatant solution became transparent. To extract natural fats, waxes, and low molecular weight lignin compounds that usually block pores on the adsorbent, and to release the reactive functional groups such as hydroxyl groups [25] 10 g of the dried raw powder was mixed with 100 ml of NaOH solution (0.1 M) using a magnetic stirrer for a period 8 h. Then the resulting mixture was filtered and washed for several times with distilled water to remove the excess NaOH and to neutralize the prepared adsorbent. Finally, the material obtained was oven-dried and passed through 230-mesh sieves to collect the particle sizes of less than 100 μm.

RESULTS AND DISCUSSION

Characterization of Raw and Dye-loaded WNS

SEM and FESEM are primary tools for characterizing the surface morphology of the prepared adsorbent. As it can be seen in Fig. 1a, the raw WNS has some cavities within which dyes could be trapped and adsorbed. This structural feature of the adsorbent increases its surface area. After chemical treatment (Figs. 1b and 1c), the size of these cavities increased.

The specific surface area for NMWNS (2.095 m^2 g^{-1}), calculated using the Brunauer-Emmett-Teller (BET) equation, is 2.3 times as much as that for WNS (0.891

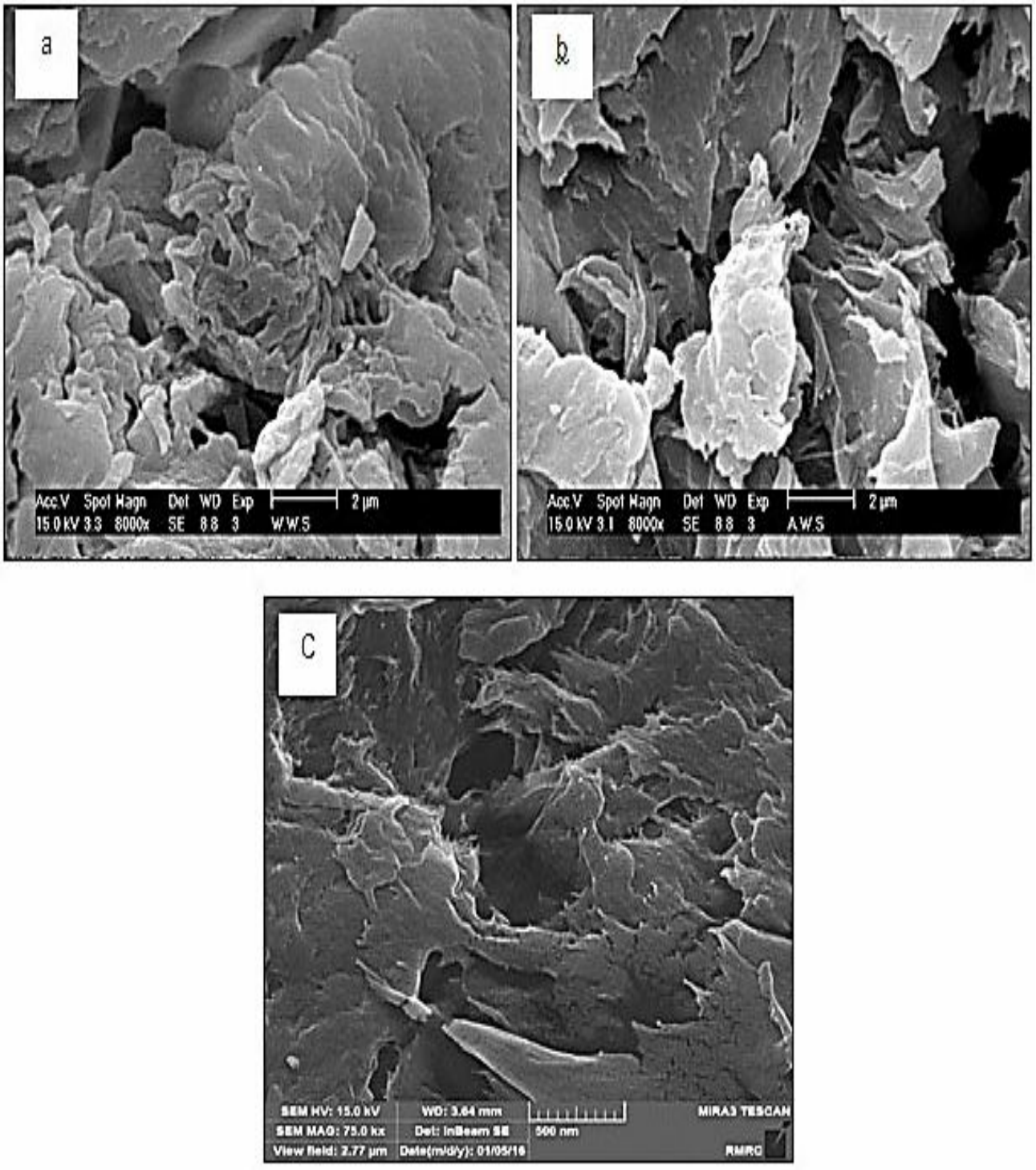

Fig. 1. (a) SEM image for raw WNS, (b) SEM image for NMWNS, and (c) FESEM for NMNS.

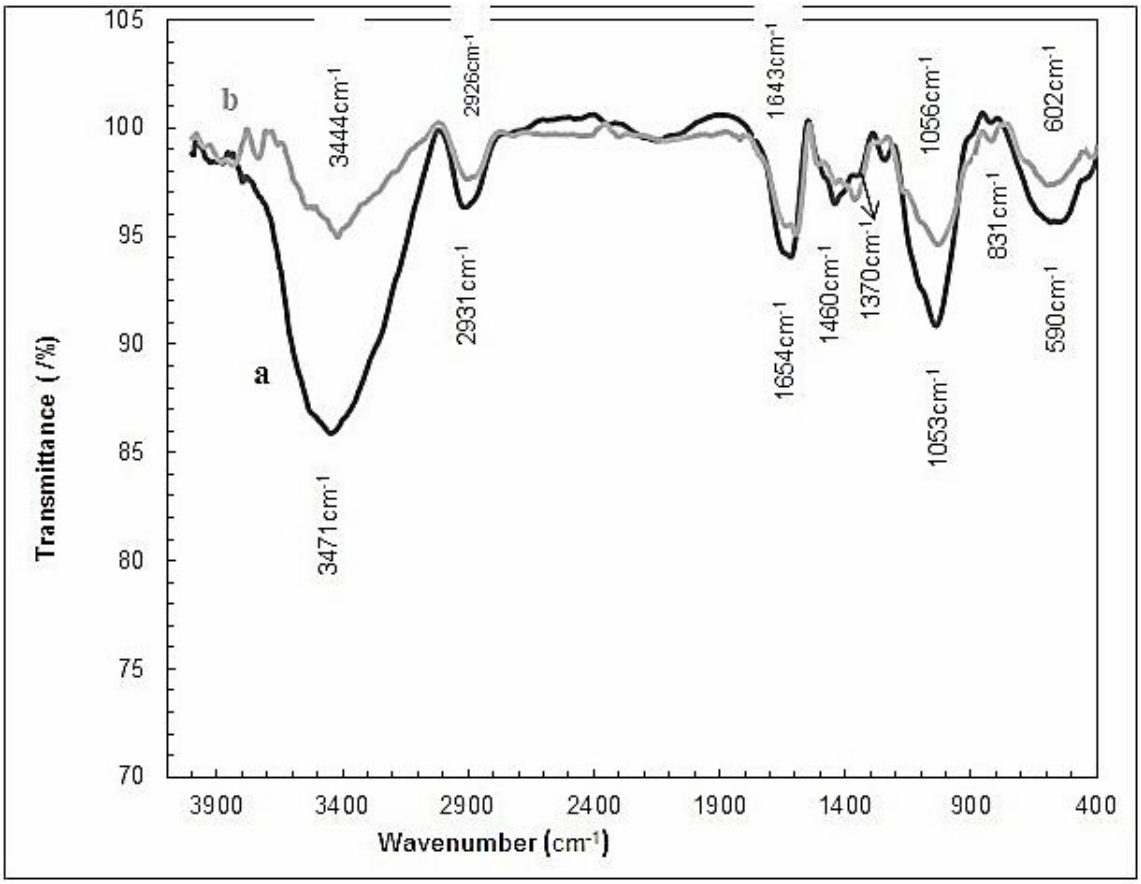

Fig. 2. FT-IR spectra for (**a)** raw and **(b)** dye-loaded NMWNS.

m^2 g^{-1}) and can provide a larger contact area to adsorb more dye molecules. Moreover, the average pore diameter of NMWNS is 32.64 nm, indicating that NMWNS is a mesoporous material.

In order to confirm the existence of functional groups on NMWNS and adsorption mechanism between the adsorbent and the adsorbate [26], the FT-IR spectra for NMWNS and dye-loaded NMWNS (Fig. 2) were recorded in the range of 400-4000 cm^{-1}. Before adsorption (Fig. 2a), the broad band at around 3471 cm^{-1} is attributed to the O-H stretching vibration of the hydroxyl groups in cellulose [27]. The well-defined peaks at 2931, 1370 and 1460 cm^{-1} are characteristics of the C-H bond stretching and bending vibrations in methyl and methylene groups, respectively [28]. The peak around 1654 cm^{-1} represents the COO group [29]. The strong C-O band at around 1053 cm^{-1} is assigned to the cellulose and lignin structures [28,30]. The bands observed at about 831 cm^{-1} could be assigned to the out-of-plane deformation of C-H [31]. As seen in Fig. 2b, after dye loading onto the adsorbent, some new peaks appeared. For example, the peak at 1590 cm^{-1} is attributed to the C=C group of the dye [29,32,33], confirming the occurrence of the adsorption process. On the other hand, some peaks were shifted or their energies were reduced (especially for the carboxyl and hydroxyl groups). These observations confirm the interactions of the dye molecules with the functional groups of the NMWNS in the adsorption process [26,27].

Determination of Zero-point Charge of NMWNS

The pH of zero-point charge (pH_{zpc}) is an important property indicating the electrical neutrality of the adsorbent

Table 1. Physico-chemical Parameters for WNS and NMWNS

Adsorbent	BET surface area ($m^2\ g^{-1}$)	Total pore volume ($cm^3\ g^{-1}$)	Mean pore diameter (nm)	Micropore Volume ($cm^3\ g^{-1}$)
WNS	0.891	0.006	26.75	0.204
NMWNS	2.095	0.0171	32.64	0.481

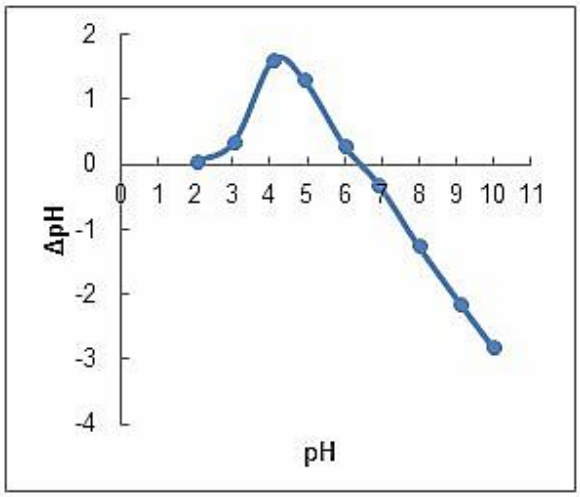

Fig. 3. Determination of pH_{ZPC} for NMWNS.

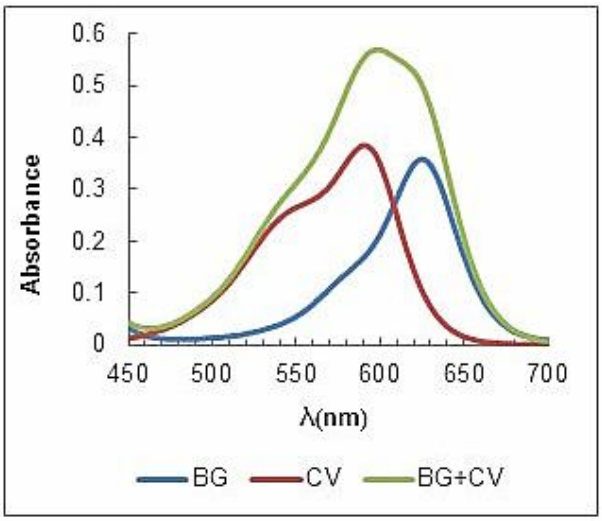

Fig. 4. Zero-order absorption spectra for BG and CV in single and binary solutions.

surface at a particular pH value [34]. The isoelectric point charge of the adsorbent was determined using the pH drift method reported in Elsevier [9]. NMWNS (4 mg) was mixed with 50 ml of potassium nitrate (0.1 M). The pH value for the mixture was adjusted to 3-10 by the addition of HCl (1.0 M) or NaOH (1.0 M). The mixture was then stirred magnetically for a period of 24 h. Then, the final pH of each suspension was measured using a pH-meter. Subsequently, the ΔpH (pH_f - pH_i) values were plotted against the initial pH values (Fig. 3). The point at which ΔpH becomes zero is called pH_{ZPC}. In this work, pH_{zpc} for NMWNS was found to be 6.5.

Simultaneous Analysis of BG and CV in Their Binary Mixture

For the simultaneous analysis of BG and CV, a binary mixture of these dyes was prepared, and the zero-order absorption spectra were recorded (Fig. 4). As one can see in this figure, due to the spectral overlapping, an accurate determination of BG and CV in their binary mixture was not possible by the direct UV-Vis absorbance measurement. In order to overcome this problem, the PLS multivariate calibration method was used. A calibration set of 35 samples was prepared. The concentration of each dye in the standard solutions lied in its the linear dynamic range. This subset was used to optimize the number of latent variables. The second subset (external test set with 8 samples) was employed for validation of the constructed model. The combination of the calibration and the prediction standards was demonstrated in Tables 2 and 4, respectively.

The optimum number of latent variables (score or factors) for each dye was determined using the leave-one-out cross-validation technique and minimization prediction error sum of squares (PRESS), and the relative error of prediction (REP) was selected as a criterion in the optimization process. These statistical parameters are defined as follow:

$$PRESS = \sum_{i=1}^{N} (\hat{C}_i - C_i)^2 \quad (3)$$

$$REP = \frac{100}{\overline{C}} \sqrt{\frac{\sum_{i=1}^{N} (\hat{C}_i - C_i)^2}{N}} \quad (4)$$

where C_i is the theoretical concentration of the analyte i, $\hat{C}_i$ is the estimated (predicted) concentration of the analyte i, $\overline{C}$ is the mean actual concentration in the calibration set, and N is the number of calibration samples. In this regard, PRESS and REP were calculated for the first latent variable, which built the PLS modeling in the calibration step. Then the second latent variable was added and PRESS was computed again. For 1-19 latent variables (half the number of standards plus one [14]), the computations were reiterated. The number of latent variables giving the minimum PRESS and REP was chosen for modeling. This process was applied for each dye in the prediction solutions, and the optimum number of latent variables was estimated. In our particular case, the number of latent variables of 2 and 3 was acquired as the optimum value for BG and CV, respectively. Also for comparing the influence of DOSC on the PLS prediction ability, the number of DOSC components changed within 1-5. Then, the original spectral data (calibration and prediction sets) was corrected using this pre-processing method. Eventually, the DOSC-corrected spectral data was directly used for the calibration and test sets. The values for PRESS and REP in the optimum number of factors obtained by applying the PLS and DOSC-PLS methods to the calibration samples were tabulated in Table 3. In continuation, the accuracy of the PLS and DOSC-PLS methods was checked using the external test that was not present in the calibration set. Different parameters such as recovery (%), relative error (E, %), and mean absolute error (MAE) were computed using Eqs. (5)-(7), respectively, and the results obtained were tabulated in Tables 4 and 5.

$$\text{Recovery} = \frac{\hat{C}_i}{C_i} \times 100 \quad (5)$$

$$Error(\%) = \frac{\hat{C}_i - C_i}{C_i} \times 100 \quad (6)$$

$$MAE = \frac{\sum_{i=1}^{n} \left| \hat{c}_i - c_i \right|_i}{n} \quad (7)$$

The values for these parameters show that by applying DOSC to the calibration and test data for each analyte, the prediction error is minimized (especially for BG) to a large

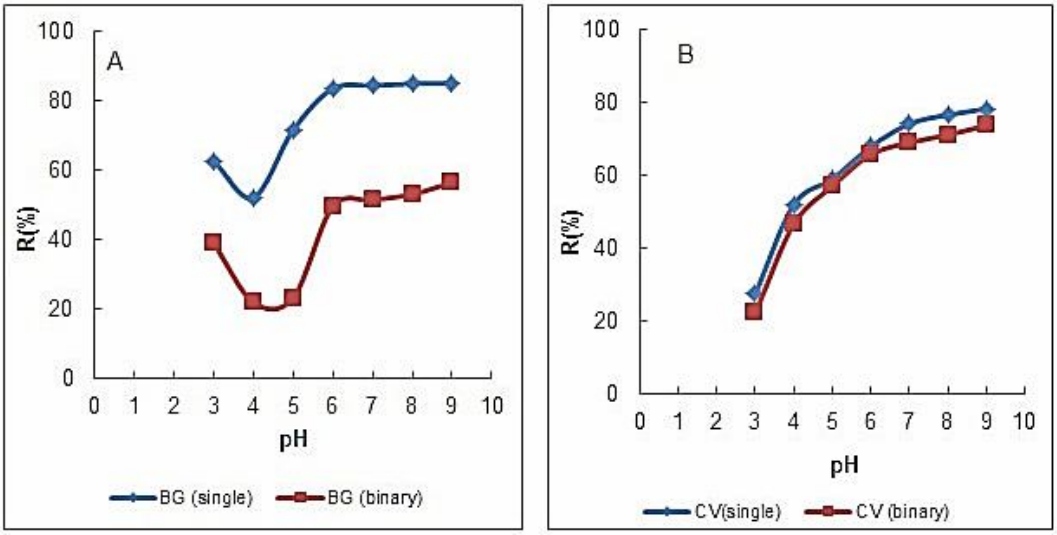

Fig. 5. Effect of pH on percentage dye removal of (A): BG and (B): CV with 0.02 g NMWNS (50 ml of 50 mg l^{-1} of dye concentration at 25 ± 2 °C) in single and binary systems.

extent. Therefore, for the subsequent experiments, the DOSC-PLS method was used to determine the BG and CV concentrations in the binary mixtures.

Effect of Initial pH on Adsorption of BG and CV in Single and Binary Systems

Since pH of the solution can affect the surface charge of the adsorbent as well as the ionization degree of the adsorbate, it is considered as a key parameter in the adsorption procedure [30,35]. In this work, the effect of initial pH value on the adsorption of dyes onto NMWNS in single and binary solutions was investigated by mixing 50 ml of 50 mg l^{-1} of the dye solutions with 0.02 g of NMWNS at various pH values in the range of 3-9, and the percentage of their removal at certain time intervals was given in Fig. 5. According to the results obtained, adsorption of the dyes onto the NMWNS is controlled by a pH-dependent mechanism. This behavior, which is also in agreement with other reported results [7,29,34] can be explained based on the structure of the dye molecules and pH_{ZPC} of the adsorbent [7,35]. The pH_{ZPC} of NMWNS was around 6.5 (Fig. 3). At pH < pH_{ZPC}, due to the high concentration of H_3O^+ ions and competition between the H^+ ions and the dye compounds for occupancy of the adsorbent active sites, the adsorbent surface becomes positive. This effect leads to ionic repulsions between the protonated adsorbent and the cationic dye molecules. Consequently, the removal percentage decreased. In contrast, at pH values higher than pH_{ZPC}, since the H_3O^+ concentration in the solution decreases and the adsorbent surface is negative, the electrostatic interaction between the cationic dye molecules and the negatively charged sites of the adsorbent leads to an increase in the dye uptake. Thus, the following reactions probably takes place at the solid/liquid interface [7,29]:

$$NMWNS\ (s) + H^+\ (aq) \rightarrow (NMWNS)H^+\ (s)$$

$$(NMWNS)H^+\ (s) + BG^+\ (aq) \rightarrow (\text{electrostatic repulsion at } pH < pH_{ZPC})$$

$$(NMWNS)H^+\ (s) \leftrightarrow BG^+\ (aq)$$

$$NMWNS\ (s) + OH^-\ (aq) \rightarrow (NMWNS)OH^-\ (s)$$

$$(NMWNS)OH^-\ (s) + BG^+\ (aq) \rightarrow (NMWNS)OH^- \ldots BG^+\ (s) \quad (\text{electrostatic interaction at } pH > pH_{ZPC})$$

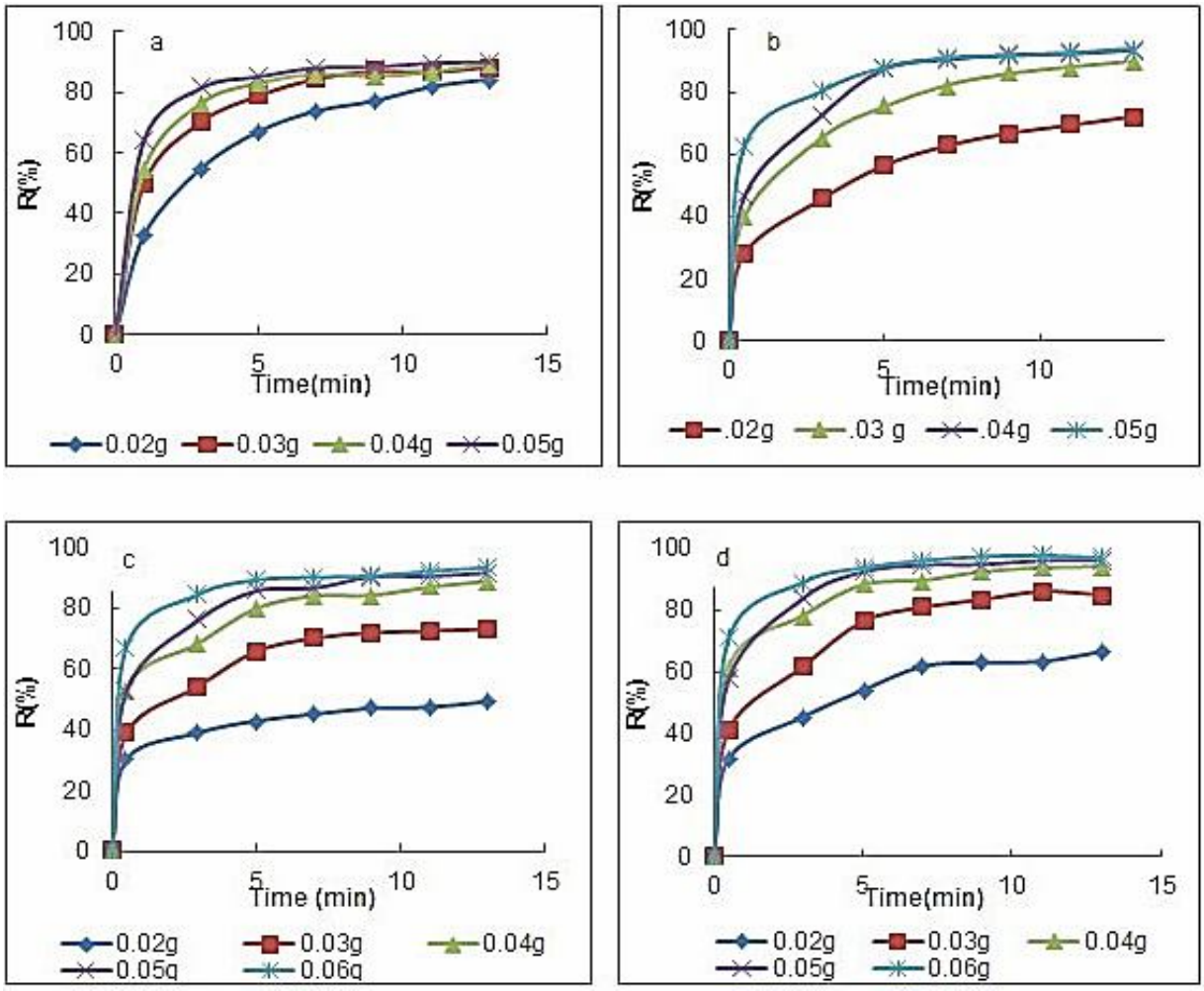

Fig. 6. Effect of adsorbent dosage on percentage of dye removal at various time intervals (50 ml of 50 mg l^{-1} of dye concentration at 25 ± 2 °C and pH = 7): a: BG (single), b: CV (single), c: BG (binary), and d: CV (binary).

Thus for the subsequent adsorption experiments, the pH of the dye solution was set at 7, at which approximately maximum removal occurred for both dyes, and it was also close to the pH value for the natural aqueous solutions, which is an advantage [36].

Effect of Adsorbent Dosage on Adsorption of Dyes in Single and Binary Systems

The effect of the NMWNS dosage on the dye removal was investigated by mixing 50 ml of 50 mg l^{-1} of dye solution at pH = 7 with various amounts of NMWNS in the single and binary systems. Plots of the removal percentage *vs.* the adsorbent dosage for the single and binary systems are illustrated in Figs. 6a-d. As it can be appreciated in these figures, the percentage of dye removal increases with increase in the adsorbent dosage up to 0.04 g, and then it approximately reaches a constant value. This is due to the greater availability of the active sites or surface area at higher concentrations of the adsorbent [37]. Therefore, the optimum adsorbent dosage of 0.04 g was selected for

Table 2. Combination of Different Mixtures of BG and CV Used in Calibration Set

Sample	BG ($mg\ l^{-1}$)	CV ($mg\ l^{-1}$)	Sample	BG ($mg\ l^{-1}$)	CV ($mg\ l^{-1}$)
1	2	2	22	8	0
2	4	8	23	8	2
3	6	0	24	6	10
4	2	8	25	8	4
5	10	4	26	10	0
6	4	4	27	10	10
7	0	4	28	0	2
8	6	8	29	10	6
9	8	6	30	2	10
10	0	10	31	8	8
11	2	0	32	2	4
12	4	2	33	4	10
13	6	6	34	0	6
14	6	4	35	10	2
15	10	8			
16	0	8			
17	2	6			
18	4	0			
19	6	2			
20	8	10			

Table 3. Values for PRESS and REP Obtained for Calibration Set by Applying Leave-one-out Cross-validation Method

Parameter	PLS		DOSC-PLS	
	BG	CV	BG	CV
PRESS	4.71	0.95	3.83	0.25
REP	7.1	3.17	6.43	1.63
Latent variable	2	3	2	2

Table 4. Values for Percentage Recovery and Relative Error for CV and BG Obtained by PLS Method

Theoretical ($mg\ l^{-1}$)		Measurement ($mg\ l^{-1}$)		Recovery (%)		Error (%)	
C_{BG}	C_{CV}	C_{BG}	C_{CV}	C_{BG}	C_{CV}	C_{BG}	C_{CV}
2.00	2.50	2.20	2.76	110.00	110.40	10.00	10.40
3.00	3.00	3.25	2.91	108.34	97.00	8.34	-3.00
5.00	5.00	5.40	5.06	108.00	101.2	8.00	1.20
0.00	5.00	-	5.12	-	102.40	-	2.40
7.00	7.00	6.39	7.25	91.28	103.57	-8.71	3.57
7.00	0.00	6.68	-	95.42	-	-4.57	-
0.00	7.00	-	7.04	-	100.57	-	0.57
9.00	9.00	8.35	9.17	92.78	101.88	-7.22	1.88
MAE						0.40	0.14

Table 5. Values for Percentage Recovery and Relative Error for CV and BG Obtained by DOSC- PLS Method

Theoretical ($mg\ l^{-1}$)		Measurement ($mg\ l^{-1}$)		Recovery (%)		Error (%)	
C_{BG}	C_{CV}	C_{BG}	C_{CV}	C_{BG}	C_{CV}	C_{BG}	C_{CV}
2.00	2.50	1.96	2.62	98.00	104.80	-2.00	4.80
3.00	3.00	3.06	2.95	102.00	98.33	2.00	-1.67
5.00	5.00	5.18	4.93	103.60	98.60	3.60	-1.40
0.00	5.00	-	4.81	-	96.20	-	-3.80
7.00	7.00	6.61	6.98	94.42	99.71	-5.57	-0.28
7.00	0.00	6.79	-	97.00	-	-3.00	-
0.00	7.00	-	7.04	-	100.57	-	0.57
9.00	9.00	8.60	9.13	95.67	101.44	-4.44	1.44
MAE						0.21	0.088

Table 6. Comparison of Individual Adsorbed Amount and Removal pprecentage at Equilibrium Found at Increasing Initial Concentration of CV and BG in the Absence and Presence of other Dyes

$C_{0,CV}$ (mg l^{-1})	$C_{0,BG}$ (mg l^{-1})	$C_{e,CV}$ (mg l^{-1})	$C_{e,BG}$ (mg l^{-1})	$q_{e,CV}$ (mg g^{-1})	$q_{e,BG}$ (mg g^{-1})	R_{CV} (%)	R_{BG} (%)
19.38	0.00	0.37	0.00	23.76	0.00	98.09	0.00
38.63	0.00	1.55	0.00	46.35	0.00	95.99	0.00
60.49	0.00	3.47	0.00	71.27	0.00	94.26	0.00
79.44	0.00	7.16	0.00	90.35	0.00	90.99	0.00
99.84	0.00	13.96	0.00	107.35	0.00	86.02	0.00
0.00	20.09	0.00	1.37	0.00	23.39	0.00	93.18
0.00	38.95	0.00	2.84	0.00	45.13	0.00	92.71
0.00	60.77	0.00	6.12	0.00	68.31	0.00	89.93
0.00	76.02	0.00	9.5	0.00	83.14	0.00	87.50
0.00	100.55	0.00	16.69	0.00	104.82	0.00	83.40
19.01	21.47	0.73	1.68	22.86	24.74	96.16	92.189
39.16	41.70	2.00	4.84	46.45	46.07	94.89	88.39
60.09	56.01	4.40	9.4	69.61	58.26	92.68	83.22
81.13	83.92	14.27	28.71	83.57	69.01	82.41	65.79
100.19	104.90	29.38	45.59	88.51	74.14	70.67	56.54

NMWNS for the single and binary systems of BG and CV.

Effect of Initial Dye Concentration on Adsorption of BG and CV in Single and Binary Systems

The effect of the initial dye concentration on the adsorption of BG and CV in single and binary systems onto the prepared adsorbent was studied by changing the initial concentration of BG and CV from 20 to 100 mg l^{-} in single and binary systems. For each experiment, the pH and adsorbent dosage were set at 7 and 0.04 g, respectively. The individual removal percentage and the individual adsorbed amount of dye at equilibrium were computed based on Eqs. (1) and (2), and the results obtained were tabulated in Table 6.

To study the effect of the initial dye concentration on the adsorption of BG and CV in their binary system, their mixture was prepared with the same concentration of BG and CV. For example, 40 mg l^{-} of BG and 40 mg $l^{-}1$ of CV were used as a mixture. After adjusting the solution pH to 7 and addition of 0.04 g of the adsorbent to 50 ml of the cited mixture, the individual percentage of removal and the individual adsorbed amount of dye at equilibrium were obtained based on Eqs. (1) and (2), and the results obtained were tabulated in Table 6. As it can be realized from this table, the individual removal percentage and the adsorbed amount of a dye at equilibrium decrease with increase in the

initial concentration of the other dye present in the mixture. For example, in the adsorption of BG in a single solution, with rise in the initial BG concentration to 100 mg l^{-1}, the adsorbed amount of BG increased to 104.82 mg/g. However, in the identical concentration range and in the presence of 100 mg l^{-1} of initial CV concentration, the adsorbed amount of BG was obtained to be 74.14 mg g^{-1}. The same trend was observed for the adsorption of the other dye (CV) onto the adsorbent in the presence of BG.

Adsoption Isotherms in Mono-component Aqueous Solutions

A successful application of the adsorption technique demands studies based on various adsorption isotherms [5]. An adsorption isotherm is basically important to describe the relationship between the amount of adsorbate uptaken by the adsorbent and the adsorbate concentration remaining in the solution [8,38]. In this work, the most common isotherm models, namely the Langmuire, Freundlich, and Temkin ones were chosen to evaluate the sorption of dyes in single component aqueous solutions. The Langmuir model, which is the most frequently applied one, is based on monolayer sorption, and can be explained as follows [39]:

$$q_{eq} = \frac{q_{\max} k_1 c_e}{1 + k_1 c_e} \tag{8}$$

where q_{max}, k_l, and C_e are the maximum adsorption capacity (mg g^{-1}), Langmuir constant (l mg^{-1}), and concentration of adsorbate at equilibrium (mg l^{-1}), respectively.

The emperical Fruendlich isotherm was the second model employed in this work. This model, which is in the following form, describes a multi-layer adsorption on the adsorbent with a heterogeneous energy distribution of the active sites [40,41].

$$q_{eq} = k_f c_e^{\frac{1}{n}} \tag{9}$$

In this equation, the variables q_{eq}, K_f, C_{eq}, and n are the equilibrium dye uptake (mg g^{-1}), relative sorption capacity ((mg g^{-1}) (l $mmol^{-1})^{1/nF}$), equilibrium concentration of the dye (mg l^{-1}), and sorption intensity, respectively.

The last isotherm that was investigeted was the Temkin isotherm, with the following matematical form:

$$q_e = B \ln A(c_e) \tag{10}$$

where (B = RT/b) and A are the Temkin constants, which are related to the heat of sorption. In this matematical equation, due to some adsorbate-adsorbate interactions, the heat of sorption of all the molecules decrease linearly with coverage [42].

The isotherm constants of each model were calculated by the non-linear least squares method in the Matlab software (see Table 7). In this procedure, the statistical parameters of root mean square error (RMSE) and the correlation coefficient (R^2), defined by Eqs. (11) and (12), respectively, were applied as the criteria for evalution of the accuracy of the prediction and the quality of fittness of the experimental data. The model that had the lowest RMSE and the largest R^2 was chosen as the superior one.

$$RMSE = \sqrt{\frac{\sum (q_{e,\exp} - q_{e,cal})^2}{n}} \tag{11}$$

$$R^2 = 1 - \frac{\sum (q_{e,\exp} - q_{e,cal})^2}{(q_{e,\exp} - \overline{q}_{e,\exp})^2} \tag{12}$$

As it can be understood from the results obtained, the Langmuire isotherm had a greater fittness of the experimental data in a single solution (see the R^2 and RMSE values given in Table 7).

Adsoption Isotherms in Bi-component Aqueous Solutions

Due to the interferences and competitive adsorption in the multi-component dye systems, the equilibrium concentration of the adsorbate is affected by the concentration of other adsorbates in the same solution. Therefore, in this work, the competitive adsorption isotherms such as extended Langmuir isotherm [43] and the Sheindorf-Rebuhn-Sheintuch isotherm (as a Freundlich-type isotherm) [40] were utilized to fit the equilibrium data obtained in the adsorption of BG and CV in their binary mixtures. The matematical form of these isotherms can be

Table 7. Constants for Single-component Isotherms Computed by Non-linear Least Squares Method for Adsorption of BG and CV

Isotherms	Parameters	Dye	
		BG	CV
Freundlich	k_f	25.45	41.21
	n	1.95	2.65
	R^2	0.9815	0.9809
	RMSE	3.87	4.13
Langmuire	q_{max}	146.40	123.20
	k_l	0.145	0.415
	R^2	0.9972	0.9848
	RMSE	1.502	3.69
Temkin	A	32.21	23.56
	B	1.447	6.17
	R^2	0.9967	0.9837
	RMSE	2.49	14.59

Table 8. Values for Multi-component Isotherm Parameters for Adorption of BG and CV in Binary Mixture

Isotherms	Parameters	Dye	
		BG	CV
Sheindorf-Rebuhn	θ_{ij}	5.64	0.442
	R^2	0.5995	0.6562
	RMSE	11.20	14.36
Extended Langmuir	q_{max}	79.07	96.01
	$k_{f,1}$	0.283	0.4904
	$k_{f,2}$	4.82×10^{-11}	6.94×10^{-12}
	R^2	0.9806	0.9917
	RMSE	1.123	2.88

expressed by Eqs. (13) and (14), respectively. In these equations, the constants $q_{max,i}$ and $k_{a,i}$ are the maximum adsorption capacity (mg g^{-1}) and Langmuir constant (l mg^{-1}) for component 'i', obtained *via* a non-linear analysis employing the Matlab software, $k_{f,i}$ and n_i are the Freundlich isotherm constants acquired for both dyes from the corresponding single-component isotherm, θ_{ij} is the competition coefficient that illustrates the inhibition for the adsorption of component 'i' by component 'j', which is estimated by non-linear fitting, $q_{e,i}^{j}$ and C_e are the adsorbed amount of component 'i' in the presence of component 'j' and equilibrium concentration, respectively. The statistical parameters of RMSE and R^2 (Table 8) obviously confirm that the extended Langmuir isotherm can describe the equilibrium data in the binary mixture with a higher accuracy.

$$q_{eq,i} = \frac{q_{\max} k_{l,i} c_{e,i}}{1 + \sum_{i=1}^{2} k_{l,i} c_{e,i}} \tag{13}$$

$$q_{e,i}^{j} = k_{f,i} c_{e,i} (c_{e,i} + \theta_{ij} c_{e,j})^{\left(\frac{1}{n_i} - 1\right)} \tag{14}$$

Adsorption Kinetic in Mono- and Bi-component Aqueous Solutions

The kinetic of adsorption of a substrate onto an adsorbent is of great importance in understanding the mechanism of the adsorption reactions and the reactor design [44]. In this regard, the pseudo-first- and second-order-rate models are the most well-known ones used to study the adsorption kinetics of the dyes [34]. The agrement between the experimental data and the predicted data was examined by calculating the R^2 values. The pseudo-first-order equation based on the equilibtium data is generally expresed as [43,44]:

$$\ln(q_e - q_t) = \ln(q_e) - k_1 t \tag{15}$$

in which the variables q_e and q_t are the adsorbed amount of dye at equilibrium (mg g^{-1}) and at time t (min), respectively, and k_1 (min^{-1}) is the adsorption rate constant. *Via* this equation, the values for k and q_e were computed using the slope and intercept of the straight-line plots of $\ln(q_e - q_t)$ against t, respectively.

The fact that the calculated values for q_e ($q_{e,cal}$) for different concentrations of a dye in single and binary systems were very far away from the experimental ones (see Tables 9 and 10) confirms that the adsorption reaction was undoubtedly not first-order. In addition, the R^2 values for each dye was rather low indicating that a first-order reaction does not take place in the adsorption of BG and CV onto the adsorbent. Thus, it was essential to apply another model to fit the experimental data. Therefore, the adsorption data was related to the pseudo-second-order kinetic model, expressed as follows [34]:

$$\frac{t}{q_t} = \frac{1}{k_2 q_e^2} + \frac{1}{q_{et}} t \tag{16}$$

The experimental data showed a better agreement with the pseudo-second-order kinetic model for both dyes in term of $R^2 > 0.99$. Furthermore, the $q_{e,cal}$ values from the pseudo-second-order model were more consistent with the $q_{e,exp}$ values (see Tables 9 and 10). For this reason, it can be concluded that the pseudo-second-order kinetic model is more appropriate to describe the adsorption behavior of a cited dye over a time range. Similar results have been reported for the removal of BG and CV by other researchers [2,35,29].

The pseudo-first-order and second-order models could not forecast the rate limiting step of the BG and CV adsorption [45]. For this reason, the experimental data were analyzed by the intra-particle diffusion model, as follows:

$$q_t = k_d t^{\frac{1}{2}} + c \tag{17}$$

where k_d and c are the intra-particle diffusion rate constant and thickness of boundary layer, respectively. These values were acquired from the slope and intercept of the plot of q_t *vs.* $t^{1/2}$. Usually the intra-particle diffusion model contains two parts that are accredited to the phenomena such as initial surface adsorption and subsequent intra-particle diffusion [8]. If the value for c is zero (the respective plot of q_t against $t^{1/2}$ passes through the origin), then the adsorption rate is controlled by the intra-particle diffusion, whereas the plots do not pass through the origin, and this is indicative of

Table 9. Kinetic Parameters for Adsorption of BG onto Prepared Adsorbent in a Single Solution and a Binary Mixture

		Pseudo-first-order				Pseudo-second-order			Intra-particle diffusion		
C_{BG} (mg g^{-1})	C_{CV} (mg g^{-1})	$q_{e(exp.)}$	$q_{e(cal.)}$	k_1	R^2	$q_{e(cal.)}$	k_2	R^2	k_d	c	R^2
20	0	23.39	13.64	0.413	0.9510	24.21	0.09	0.9999	6.30	4.44	0.8063
40	0	45.13	18.07	0.351	0.8181	45.87	0.069	0.9998	12.03	9.16	0.7815
60	0	68.31	32.87	0.455	0.9148	69.93	0.047	0.9999	18.38	13.76	0.7865
80	0	83.14	40.58	0.399	0.8808	85.47	0.029	0.9996	22.44	15.95	0.8029
100	0	104.81	67.90	0.431	0.9495	109.89	0.015	0.9995	28.64	18.40	0.8309
40	40	46.07	44.97	0.563	0.9756	48.31	0.025	0.9995	12.48	7.20	0.8573
100	100	74.14	53.37	0.289	0.9642	76.92	0.008	0.9989	19.16	9.07	0.8988

Table 10. Kinetic Parameters for Adsorption of CV onto Prepared Adsorbent in a Single Solution and a Binary Mixture

		Pseudo-first-order				Pseudo-second-order			Intra-particle diffusion		
C_{CV} (mg g^{-1})	C_{BG} (mg g^{-1})	$q_{e\ (exp.)}$	$q_{e\ (cal.)}$	k_1	R^2	$q_{e\ (cal.)}$	k_2	R^2	k_d	c	R^2
20	0	23.76	16.14	0.5944	0.9530	24.10	0.140	0.9999	6.33	4.78	0.7842
40	0	46.35	31.82	0.4616	0.9697	48.54	0.037	0.9998	12.62	8.41	0.8223
60	0	71.27	69.41	0.4868	0.8880	75.75	0.017	0.9995	19.55	11.82	0.8470
80	0	90.35	68.03	0.3570	0.9762	98.04	0.0093	0.9998	24.81	13.39	0.8744
100	0	107.35	85.63	0.3816	0.9888	114.94	0.0085	0.9999	29.39	16.52	0.8663
40	40	46.50	33.11	0.3915	0.9719	49.50	0.024	0.9997	12.76	7.48	0.8546
100	100	88.51	95.15	0.466	0.9971	91.20	0.0083	0.9986	24.35	12.28	0.8843

some degree of boundary layer control, and shows that the intra-particle diffusion is not the only rate limiting step [8, 46]. Based on the results obtained (see Tables 9 and 10), adsorption onto the studied adsorbent was affected by more than one process.

Comparison with Previously Developed Adsorbents for Adsorption of BG and CV

A comparison assesment between the efficiency of different adsorbents for the cationic dyes BG and CV is illustrated in Table 11. As Table 11 shows, the present work is superior or comparable to the previously reported ones.

Table 11. Comparison between the Adsorption Capacity of Various Reported Adsorbents for Removal of MB and CV

Adsorbent	Dye	q_m (mg g^{-1})	Conc. (mg l^{-1})	Contact time	pH	Ref.
Red clay	BG	125	20-100	1600 min	7	[47]
Activated carbon	BG	273	20-1500	360 min	5.5	[48]
Saklikent mud	BG	1.18	1-20	480 min	6.5	[49]
Acron	BG	2.1	10-50	40 min	6	[35]
NMWNS	BG	146.4	20-100	13 min	7	This work
Wheat straw	CV	227.27	50-700	120 min	7	[50]
$CaFe_2O_4$	CV	0.87	10-120	30 min	7	[6]
Magnetic tea waste	CV	113.64	NR	45 min	10	[34]
Coniferous pinus bark	CV	32.78	10-50	180 min	8	[37]
NMWNS	CV	123.2	20-100	13 min	7	This work

NR: Not reported.

Possible Mechanism

In general, the structure of an adsorbate and the surface properties of an adsorbent are the factors that can affect the sorption behavior [29,51]. Both dyes, due to dissociation in water, produce nitrogen with a positive charge (N^+). On the other hand, as seen in the FT-IR spectrum, there are different functional groups such as the carboxyl and hydroxyl groups on the adsorbent. The pH examination showed that the adsorption process was dependent on the electrostatic forces. Therefore, based on the results obtained and the structure of the adsorbate and adsorbent, the possible mechanism may be [51]:

(i): Transportation of the dye species from the bulk of the solution toward the surface of NMWNS.

(ii): Transmission of the dye species *via* the boundary layer to the surface of NMWNS.

(iii): Aggregation of the dye species on the surface of NMWNS based on the Van der Waals forces or hydrophobic-hydrophobic forces between the hydrophobic parts of the dyes and NMWNS or the electrostatic interaction between the positively charged N^+ of the dyes and electron-rich sites (negatively charged surface of NMWNS) or based on the FT-IR spectrum, the formation of hydrogen bond between nitrogen atoms in the structure of dye and -OH and -COOH groups on the surface of NMWNS.

(iv): Intra-particle diffusion of dye species into the interior pores of NMWNS.

Therefore, based on these reasons, one can conclude that both the physical and chemical interactions are responsible for adsorption of the understudied dyes.

Reuse of the Prepared Adsorbent

Reusability of the adsorbent is very important in practical applications [52]. An efficient adsorbent should have both high adsorption capacities and excellent desorption characteristics in order to make the wastewater treatment economic [52,6]. Therefore, to examine the possibility of reusing the NMWNS beads, desorption studies were carried out using a 10% solution of sodium dodecyl sulfate (SDS) and a dish-washing liquid as the eluent solvents. In this regard, 40 ml of distilled water was added to 0.7 g of exhausted NMWNS. Then a few drops of a dish-washing liquid were added to the mixture, and the mixture was stirred for 30 min. After that, the adsorbent was washed with distilled water. This procedure was repeated for the regeneration of adsorbent by SDS. Then, 0.04 g of the dried adsorbent was used for the removal of 50 ml of 50 ppm of the dye at pH = 7. Interestingly, the results obtained showed that approximately 90% of the dye could be adsorbed using NMWNS, recovered by means of the dish-washing liquid or SDS in the first cycle of regeneration. These result confirmed the presence of electrostatic interactions between the adsorbent and the adsorbate. Therefore, in the next cycles, the dish-washing liquid was used, as a cheap and available solvent, for the regeneration of exhausted adsorbent. It was found that in 5 cycles, the NMWNS results were almost the same as those obtained in the first regeneration cycle.

This study focused on the utilization of NMWNS for the removal of the BG and CV dyes from a single solution and a binary mixture. The operational factors including pH, adsorbent dosage, initial dye concentration, and contact time were found to affect the removal percentage of the cited dyes. The removal percentage of the dye molecules increased with increase in the pH, adsorbent dose, and contact time. On the other hand, it decreased with an increase in the initial dye concentration. NMWNS is a low-cost and available adsorbent with a high surface area. The FT-IR analysis revealed that the OH and COOH functional groups are responsible for the adsorption process. The facile and rapid adsorption of dyes are attributed to the NMWNS high surface area and the functional groups present on it. The equilibrium data using different isotherms demostrated that the nature of the cited dyes adsorbed onto NMWNS was more compatible with the Langmuire model. The results obtained for the kinetic data by the two models pseudo-first-order and pseudo-second order showed that adsorption of the studied dyes onto NMWNS followed a pseudo-second-order kinetic. Also, the efficiency of NMWNS was compared with that of some other adsorbents examiend in the removal of BG and CV from aqueous solutions. The results obtained confirm that NMWNS is comparable or better than some of the adsorbents in term of the high adsoption capacity and the short time required for removal of the dyes. However, to apply this environmentally friendly adsorbent in industrial processes for the removal of contaminants from textile industry effluents, continuous column studies are required to be performed.

ACKNOWLEDGMENTS

The authors are thankful to the Shahrood University of Technology Research Council for the support of this work.

REFERENCES

[1] M. Arshadi, A. Faraji, M. Amiri, M. Mehravar, A. Gil, J. Colloid. Interface Sci. 446 (2015) 11.

[2] M. Ghaedi, S. Hajati, B. Barazesh, F. Karimi, G. Ghezelbash, Ind. Eng. Chem. Res. 19(2013) 227.

[3] S.R. Shirsath, A.P. Patil, R. Patil, J.B. Naik, P.R. Gogate, S.H. Sonawane, Ultrason. Sonochem. 20 (2013) 914.

[4] A. Saeed, M. Sharif, M. Iqbal, J. Hazard. Mater. 179 (2010) 564.

[5] A. Shokrollahi, A. Alizadeh, Z. Malekhosseini, M. Ranjbar, J. Chem. Eng. Data 56 (2011) 3738.

[6] S. An, X. Liu, L. Yang, L. Zhang, Chem. Eng. Res. Des. 94 (2015) 726.

[7] A. Kurniawan, H. Sutiono, N. Indraswati, S. Ismadji, J. Chem. Eng. 189 (2012) 264.

[8] N.M. Mahmoodi, R. Salehi, M. Arami, Desalination

272 (2011) 187.
[9] R. Slimani, I. El Ouahabi, F. Abidi, M. El Haddad, A. Regti, M.R. Laamari, S. El Antri, S. Lazar, J. Taiwan Inst. Chem. Eng. 45 (2014) 1578.
[10] P. Sharma, H. Kaur, M. Sharma, V. Sahore, J. Environ. Monit. Assess. 183 (2011) 151.
[11] S. Saadat, A. Karimi-Jashni, Chem. Eng. J. 173 (2011) 743.
[12] M.K. Dahri, M.R.R. Kooh, L.B. Lim, J. Environ. Chem. Eng. 2 (2014) 1434.
[13] A. Çelekli, S.S. Birecikligil, F. Geyik, H. Bozkurt, Bioresour. Technol. 103 (2012) 64.
[14] J.-F. Gao, J.-H. Wang, C. Yang, S.-Y. Wang, Y.-Z. Peng, Chem. Eng. J. 171 (2011) 967.
[15] J.B. Nevado, J.R.G. Flores, M.V. Llerena, N.R.G. Fariñas, Talanta 48 (1999) 895.
[16] S. Wold, M. Sjöström, L. Eriksson, Chemom. Intell. Lab. Syst. 58 (2001) 109.
[17] M.A. Chamjangali, G. Bagherian, G. Azizi, Spectrochim. Acta Part A 62 (2005) 189.
[18] A. Niazi, A. Yazdanipour, J. hazard. Mater. 146 (2007) 421.
[19] S. Wold, H. Antti, F. Lindgren, J. Öhman, Chemom. Intell. Lab. Syst. 44 (1998) 175.
[20] D. Zhu, B. Ji, C. Meng, B. Shi, Z. Tu, Z. Qing, Chemom. Intell. Lab. Syst. 90 (2008) 108.
[21] K. Zarei, M. Atabati, Z. Malekshabani, Anal. Chim. Acta 556 (2006) 247.
[22] J.A. Westerhuis, S. de Jong, A.K. Smilde, Chemom. Intell. Lab. Syst. 56 (2001) 13.
[23] J. Luypaert, S. Heuerding, S. De Jong, D. Massart, J. Pharm. Biomed. Anal. 30 (2002) 453.
[24] A. Lorber, L.E. Wangen, B.R. Kowalski, J. Chemom. 1 (1987) 191.
[25] M.T. Yagub, Removal of Methylene Blue Contaminant by Natural and Modified Low Cost Agricultural By-product, in Curtin University, 2013.
[26] M. Peydayesh, A. Rahbar-Kelishami, Ind. Eng. Chem. Res. 21 (2015) 1014.
[27] T. Akar, I. Tosun, Z. Kaynak, E. Ozkara, O. Yeni, E.N. Sahin, S.T. Akar, J. Hazard. Mater. 166 (2009) 1217.
[28] J.-S. Cao, J.-X. Lin, F. Fang, M.-T. Zhang, Z.-R. Hu, Bioresour. Technol. 163 (2014) 199.
[29] R. Kumar, R. Ahmad, Desalination 265 (2011) 112.
[30] J.-Z. Guo, B. Li, L. Liu, K. Lv, Chemosphere 111 (2014) 225.
[31] J. Yang, K. Qiu, Chem. Eng. J. 165 (2010) 209.
[32] S. Jain, R.V. Jayaram, Desalination 250 (2010) 921.
[33] E. Cho, M.N. Tahir, H. Kim, J.-H. Yu, S. Jung, RSC Adv. 5 (2015) 34327.
[34] T. Madrakian, A. Afkhami, M. Ahmadi, Spectrochim. Acta Part A99 (2012) 102.
[35] M. Ghaedi, H. Hossainian, M. Montazerozohori, A. Shokrollahi, F. Shojaipour, M. Soylak, M. Purkait, Desalination 281 (2011) 226.
[36] Y. Zhang, J. Xu, Z. Yuan, H. Xu, Q. Yu, Bioresour. Technol. 101 (2010) 3153.
[37] [R. Ahmad, J. Hazard. Mater. 171 (2009) 767.
[38] J.-H. Deng, X.-R. Zhang, G.-M. Zeng, J.-L. Gong, Q.-Y. Niu, J. Liang, Chem. Eng. J. 226 (2013) 189.
[39] N.M. Mahmoodi, J. Taiwan Inst. Chem. Eng. 44 (2013) 322.
[40] M. Turabık, B. Gozmen, CLEAN-Soil, Air, Water 41 (2013) 1080.
[41] M.E. Fernandez, G.V. Nunell, P.R. Bonelli, A.L. Cukierman, J. Ind. Crops Prod. 62 (2014) 437.
[42] B. Hameed, J. Hazard. Mater. 162 (2009) 939.
[43] J. Zolgharnein, M. Bagtash, T. Shariatmanesh, Spectrochim. Acta Part A 137 (2015) 1016.
[44] M.R. Malekbala, M.A. Khan, S. Hosseini, L.C. Abdullah, T.S. Choong, J. Ind. Eng. Chem. 21 (2015) 369.
[45] B.H. Hameed, J. Hazard. Mater. 161 (2009) 753.
[46] M. Ghaedi, S. Hajjati, Z. Mahmudi, I. Tyagi, S. Agarwal, A. Maity, V. Gupta, Chem. Eng. J. 268 (2015) 28.
[47] M.S.U. Rehman, M. Munir, M. Ashfaq, N. Rashid, M.F. Nazar, M. Danish, J.-I. Han, Chem. Eng. J. 228 (2013) 54.
[48] T. Calvete, E.C. Lima, N.F. Cardoso, S.L. Dias, E.S. Ribeiro, Clean-Soil, Air, Water 38 (2010) 521.
[49] Y. Kismir, A.Z. Aroguz, Chem. Eng. J. 172 (2011) 199.

[50] R. Gong, S. Zhu, D. Zhang, J. Chen, S. Ni, R. Guan, Desalination 230 (2008) 220.
[51] S. Chakraborty, S. Chowdhury, P.D. Saha, Carbohydr. Polym. 86 (2011) 1533.
[52] Y. Su, B. Zhao, W. Xiao, R. Han, Environ. Sci. Pollut. Res. 20 (2013) 5558.